



# Bulletin of the Mineral Research and Exploration

<http://bulletin.mta.gov.tr>



## TECTONIC GEOMORPHOLOGY OF BAŞKALE FAULT ZONE

Azad SAĞLAM SELÇUK<sup>a\*</sup> and Meryem DÜZGÜN<sup>b</sup>

<sup>a</sup>*Yüzüncü Yıl University, Faculty of Engineering-Architecture, Department of Geological Engineering, 65080 Tuşba/Van. orcid.org/0000-0003-4943-3870*

<sup>b</sup>*Yüzüncü Yıl University, Institute of Science, 65080 Tuşba/Van. orcid.org/0000-0001-6017-2312*

Research Article

### Key words:

Başkale Fault Zone, Morphotectonic, geomorphic indices, uplift rates, the Eastern Anatolia.

### ABSTRACT

Başkale Fault Zone is located between Şemdinli-Yüksekova fault zone in southeast Turkey and Guilato-Siahcheshmeh-Khoy fault system in southeast Iran. The fault zone started from Yavuzlar town to Işıklar village in southwest. BFZ is composed of three different segments which have directions with varying N75°E to N 80°E. The offset streams, fault controlled drainage system such as Çığılsuyu stream, alluvial fans which line up parallel to the fault and have deformation structure, fault straight, Plio-Quaternary volcanic rocks and volcanic structures, ridge travertines which continues their formations today indicate that BFZ is active as morphotectonic. The objective of the investigation is to determine the effect of Başkale Fault Zone on morphotectonic evolution of the region. With this aim, morphometric indices such hypsometric integral, drainage basin asymmetry, the ratio between the width and the height of valley and crimp in front of the mountain were produced with Digital Elevation Model of study area and were explained with their meaning. Depending on the results of morphometric models, it appears that the region has young topography and actively rises. It was concluded that the rate of topographies rise in the region increased from east to west and typically rates were greater than of 0.5 mm in year.

Accepted Date: 10.07.2016

Received Date: 28.07.2016

## 1. Introduction

Başkale Fault Zone is located with the western section of the East Anatolia-Iran plateau forming the East Anatolia Compressional Tectonic Block (EACT). This block, defined by modeling of long-term GPS measurements (Reilinger et al., 2006; Djomour et al., 2011), is bounded by the left-lateral strike-slip Northeast Anatolian Fault in the northwest, by the Lesser Caucasus in the north/northeast and by the Bitlis-Zagros thrust belt in the south (Figure 1). It is proposed that the EACT developed under a N-S oriented compressional tectonic regime related to the continent-continent collision between the Arabian and Eurasian plate 13 million years ago (Şengör and Kidd, 1979; Şengör and Yılmaz, 1981; Dewey et al., 1986; Şaroğlu and Yılmaz, 1986; Yılmaz et al., 1987; Koçyiğit et al., 2001) (Figure 1). However, some studies published in recent years have stated that the tectonic regime represented by compression-shortening is only active along the Bitlis-Zagros

thrust zone and between the end of the Late Miocene and end of the Early Pliocene (Koçyiğit et al., 2001; Koçyiğit, 2013). Koçyiğit et al. (2001) stated that instead of a compressional-shortening tectonic regime in the EACT block, a compressional type of neotectonic regime ended in the Late Pliocene. Linked to this regime, NW-SE and NE-SW oriented strike-slip faults, E-W oriented reverse/thrust faults and folds, N-S oriented normal faults and N-S oriented extensional fractures determining the location of significant volcanic centers developed in the region. Among the main neotectonic structures in the region are NW-SE oriented right-lateral strike-slip faults (Çaldıran (CF), Bitlis (BF) and Erciş (KEF) faults, etc.), NE-SW oriented left-lateral strike-slip faults (Ahlat fault (AhF), Başkale (BFZ) fault zone, etc.) and almost E-W oriented thrust faults (Muş-Gevaş thrust zone, Bitlis Zagros suture zone (BZSZ), Gürpınar fault (GF) and Van fault zone (TF) etc.) (Arpat et al., 1977; Şaroğlu et al., 1984; Koçyiğit, 1985a, 1985b;

\* Corresponding author: Azad Sağlam SELÇUK, [azadsaglam@gmail.com](mailto:azadsaglam@gmail.com)  
<http://dx.doi.org/10.19111/bulletinofmre.315757>



Figure 1- Location of the study area within Turkey's neotectonic framework (block boundaries taken from Reilinger et al., 2006; Djmour et al., 2011) (NAFZ: North Anatolia Fault Zone, EAFZ: East Anatolia Fault Zone, BZSZ: Bitlis-Zagros Suture Zone, CF: Çaldıran Fault, KTF: Karllova triple junction, VFZ: Varto Fault Zone, NEAF: Northeast Anatolia Fault, EACT: East Anatolia Compressional Tectonic block).

Koçyiğit et al., 1985; Şaroğlu and Yılmaz, 1986; Saroğlu et al., 1987; Cisternas et al., 1989; Rebai et al., 1993; Koçyiğit et al., 2001; Dhont and Chorowicz, 2006; Horasan and Boztepe-Güney, 2006) (Figure 2). These faults or fault zones are the source of many destructive earthquakes occurring in the region from the historical period to the present day.

After the 23 October 2011 Van earthquake more detailed studies of the young tectonics of the Lake Van Basin have been completed by different researchers. The majority of these studies have focused on the basic properties of the main fault that produced the 2011 Van earthquake and the place of this mechanism in the geodynamic structure of the region (Özkaymak et al., 2011; Emre et al., 2012; Bayraktar et al., 2013; Görgün 2013; Doğan and Karakaş 2013; Altıner et al., 2013, Elliott et al., 2013; Koçyiğit, 2013). Some of these studies have drawn attention to the Başkale Fault Zone (BFZ), located southeast of Lake Van Basin and one of the NE-SW oriented strike-slip fault zones, as being a neotectonic structure that is active and has potential to produce earthquakes (Emre et al., 2012; Koçyiğit, 2013). Due to its active tectonic properties, the Başkale basin and Başkale Fault Zone have an important place in understanding the tectonic evolution of the region. With the active property of producing more than one earthquake proven, the BFZ has only been studied in limited fashion to date. The BFZ was only mapped after the 25 January 2005

Sütlüce earthquake (Mw 4.8, 4.9 and 5.5) (KOERİ, 2011) and is included on Turkey's Active Fault Map.

This study aimed to research the BFZ, controlling the western and eastern boundaries of the Başkale Basin, using morphometric indices such as mountain-front sinuosity ( $S_{mf}$ ), valley floor width to height ratio ( $V_f$ ), asymmetry factor (AF) and hypsometric integral (HI) and its effect on regional geomorphologic evolution.

### 1.1. Başkale Fault Zone

The Başkale basin is southeast of Lake Van; located between the BZSZ bounding the south of the lake and the Guilato–Siahcheshmeh–Khoy Fault system located in northwest Iran (Figure 2). This NE-SW striking basin has width of 9-15 km and length of 82 km (Figure 3a). The east and west sides of the Başkale basin is controlled by faults. While basement rocks are located in the footwall of these faults bounding the basin, the sediments filling the basin are generally fluvial and current alluvium. Three basic geologic units separated by unconformities may be distinguished in Başkale basin: (1) Pre-Neogene basic metamorphic rocks comprised of dominantly marble and schists (Yılmaz, 1971; Ricou, 1971; Yılmaz, 1975; Boray, 1975; Erdoğan, 1975, Göncüoğlu and Turhan, 1984); (2) Neogene continental sediments and volcanic rocks (lacustrine limestone, sandstone and basalt-

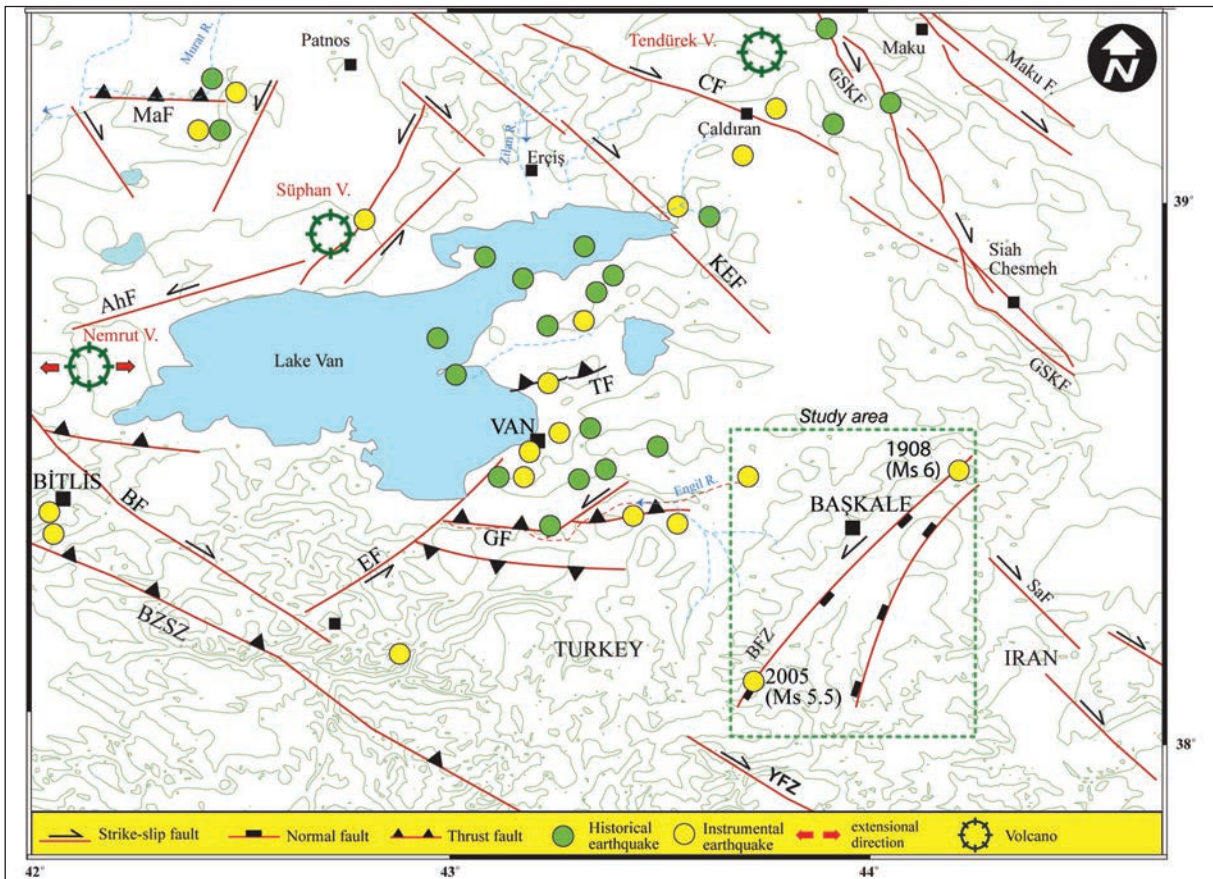


Figure 2- Seismotectonic map of the study area and surroundings (faults: Koçyiğit et al., 2001, Karakhanian et al., 2004; earthquakes Ergin et al., 1967; Soysal et al., 1981; Ambraseys and Finkel, 1995; Tan et al., 2008) (BZSZ: Bitlis-Zagros Suture Zone, MaF: Malazgirt Fault, CF: Çaldıran Fault, GSKF: Guilato-Siahcheshmeh-Khoy Fault, KEF: Karayazı-Erçiş Fault, TF: Van Fault, SaF: Salamas Fault, BFZ: Başkale Fault Zone, YFZ: Yüksekova Fault Zone, GF: Gürpınar Fault, EF: Edremit Fault, BF: Bitlis Fault, AhF: Ahlat Fault).

tuff); and (3) Quaternary alluvial, fluvial and colluvial sediments and travertine formations (Figure 3b). The contacts between units in the basin are generally fault-controlled (Figure 4a). While Quaternary sediments form the basin fill, metamorphic rocks are located in the west of the basin, while volcanic rocks are generally located along the eastern edge (Figure 3b). Travertine deposits dominantly developed along the Çamlık Fault bounding the southeast of Başkale basin (Figure 4b-c). The BFZ begins in the northeast, north of Yavuzlar, and continues until Işıklı village in the southwest (Figure 3). With strike varying from dominantly N10°E and N40°E, the BFZ is generally comprised of left lateral strike-slip faults with normal component. While the west section of the basin is controlled by two faults (Işıklı and Ziraniş faults), the east section is controlled by a single fault (Çamlık fault). One of the faults bounding the NW of the Başkale basin is the Ziraniş fault, which is nearly 20 km long with strike N5°E to N-S. This

edge of the basin is represented by a structural contact between pre-Miocene basement rocks and Quaternary alluvium (Figure 3b). The more southern Işıklı Fault may be followed for 14 km between Ortayol and Işıklı and has a right-curving geometry. South of Başkale it presents a linear strike between pre-Miocene basement rocks of marble-schist intercalations and Miocene-aged sedimentary rocks (Figure 3b). The central sections of the basin are controlled by younger normal faults compared to the faults controlling the edges and in this area they appear to have formed a stepped morphology. The Ereğ and Alabayır Faults begin in the north near Yavuzlar village and may be followed to Ilıcak village in the south. Cutting the fluvial sediments of the Çığılsu river, they form 2-3 m steps within these sediments. Çamlık Fault bounds the southeast of the basin and also controls it. With nearly 30 km length, it has strike varying from N10°-25°E. Ancient and new travertine deposits outcrop along the Çamlık Fault (Figure 4b-c). The fissure ridge

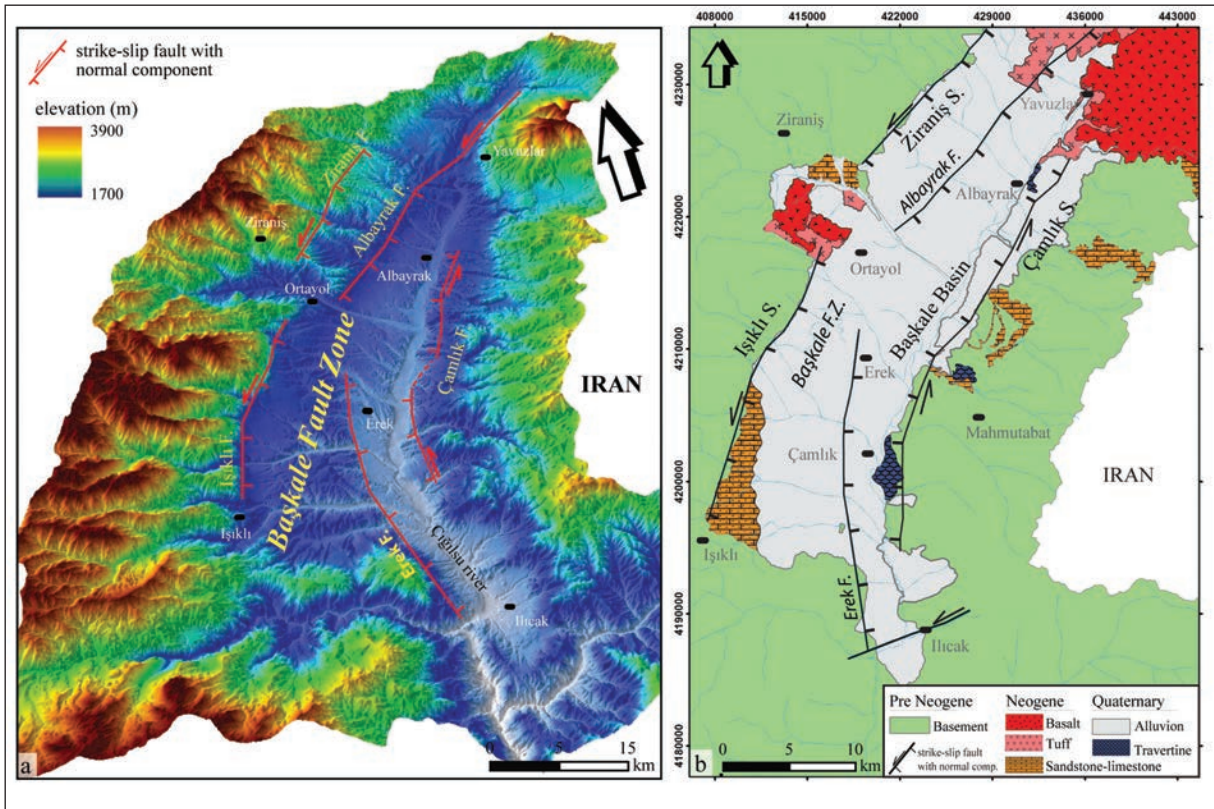


Figure 3- a) Extension of the Başkale Fault Zone on digital elevation model b) Geologic map of the Başkale basin (adapted from Ateş et al., 2007).

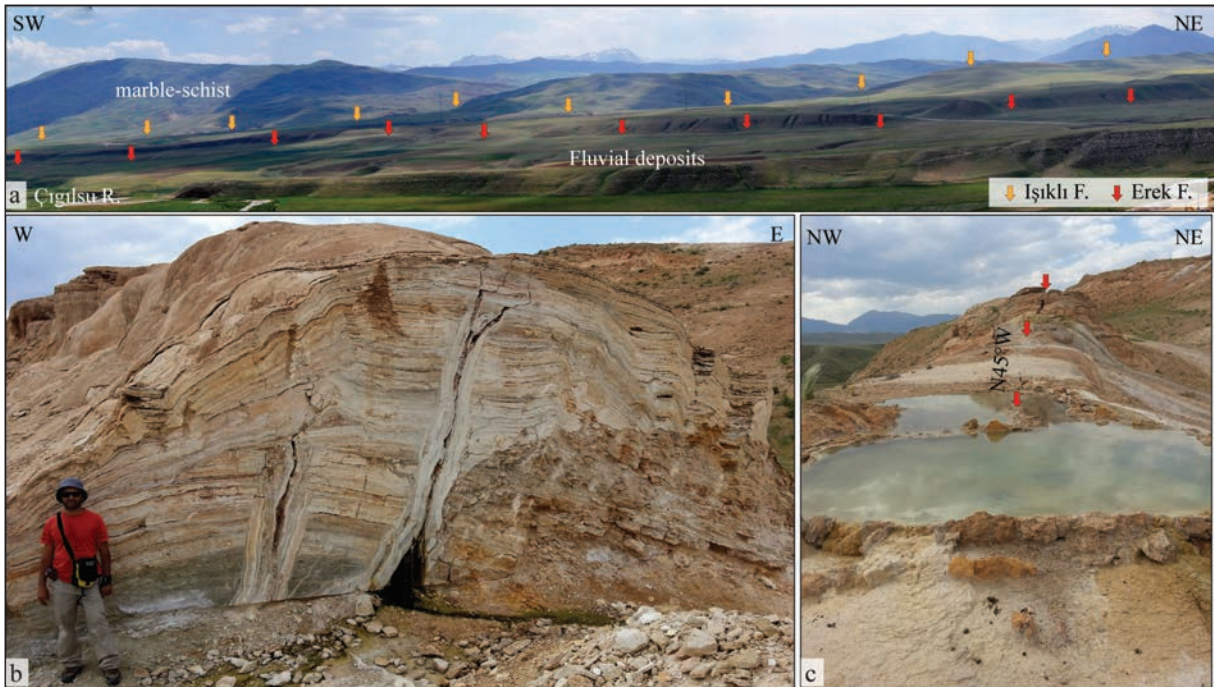


Figure 4- a) Extension of Işıklı and Ereğ Fault in the field b) Cross section of fissure ridge travertines along Çamlık Fault c) Longitudinal appearance of fissure ridge travertines

travertines and terrace-type travertines with formation continuing currently are noteworthy.

Başkale Fault Zone is a tectonically active fault zone and is the source of more than one earthquake in the instrumental period. In previous years though the Başkale Fault was described, it was named the Başkale Fault zone due to the occurrence of more than one active fault almost parallel to each other and the deformation zone occurring along these faults (Başkale basin). As proven by the 1908 Başkale earthquake (Mw 6.0) (Ambraseys and Finkel, 1995; Ambraseys, 2001) and 25 January 2005 Sütluce earthquakes (Mw 4.8, 4.9 and 5.5) (KOERİ, 2011), the BFZ is a seismically active fault zone (Koçyiğit, 2005; Emre et al., 2005, 2012).

## 2. Method

Research to date has shown that activity occurring along the fault has left different geomorphological evidence at the surface (Bull, 1977; Keller, 1986; Keller and Pinter, 2002; Gordon, 1998; Giamboni et al., 2005). One of the most commonly used methods for interpretation of this evidence is morphometric analysis. Morphometric analysis is one of the most important tools used to research the effect of tectonic activity on development of geomorphic processes and surface morphology (Keller and Pinter, 2002). This analysis is completed using morphometric indices and generally is used to describe regional tectonic activity. The obtained numerical data may be used with the aim of understanding the geomorphological evolution of large areas or determining which active fault segment is more active (Strahler, 1952; Bull and McFadden, 1977; Keller et al., 2000; Azor et al., 2002; Keller and Pinter, 2002; Font et al., 2010; Gürbüz and Gürer, 2008; Özkaymak and Sözbilir, 2012; Yıldırım, 2014; Özsayın, 2016).

For determination of the morphological characteristics of Başkale Fault Zone and to be able to complete morphometric analyses, a digital elevation model (DEM) of the study area with 10 m resolution was created using the ArcMap program. The drainage basins and fluvial network in the region were drawn on the created DEM base. Morphometric indices (mountain-front sinuosity ( $S_{mf}$ ), valley floor width to height ratio ( $V_p$ ), asymmetry factor, (AF) and hypsometric curve and integral (HE and HI) were calculated using different tools within the ArcMap program.

## 3. Morphometric Analyses

### 3.1. Mountain-front sinuosity ( $S_{mf}$ )

Mountain-front sinuosity is an effective method to distinguish tectonically active mountain fronts from inactive mountain fronts and is described by the following equation (Bull and McFadden, 1977; Keller and Pinter, 2002).

$$S_{mf} = \frac{L_{mf}}{L_s}$$

In this formula,  $L_{mf}$  is the sinuous length of the mountain front while  $L_s$  is the length of a straight line along the front.  $S_{mf}$  is a function of erosion and tectonic activity and values change linked to uplift rate (Rockwell et al., 1984). If mountain fronts are controlled by active faults, they give low  $S_{mf}$  values, while with the reduction in uplift rate and/or tectonism erosion becomes dominant and  $S_{mf}$  values increase (Keller and Pinter, 2002; Silva et al., 2003; Bull, 2007; Pérez-Peña et al., 2010).

In this study the  $S_{mf}$  values for the mountain fronts long the segments of the BFZ controlling the basin were calculated. These values generally varied between 1.0 and 2.0. The S2 and S4-S7 segments controlling the west edge and the northeast of the basin gave low  $S_{mf}$  values (in the interval 1.07-1.08; Table 1, Figure 5a and 5b) and these values show that these segments are more active in the region. The S7-8-9 segments controlling the east edge of the basin and the S3 segment located in the south gave low  $S_{mf}$  values (in the interval 1.53-1.95, Table 1, Figure 5a) and as a result the west and central segments may be described as being less active segments.

Table 1- Mountain-front sinuosity ( $S_{mf}$ ) values (for points see figure 5).

| Mountain-front | Smf  |
|----------------|------|
| S1             | 1,33 |
| S2             | 1,08 |
| S3             | 1,56 |
| S4             | 1,08 |
| S5             | 1,06 |
| S6             | 1,07 |
| S7             | 1,04 |
| S8             | 1,75 |
| S9             | 1,95 |
| S10            | 1,53 |

### 3.2. Valley floor width to height ratio ( $V_p$ )

One of the most commonly used indices to understand the tectonic uplift rate occurring in a

region is the valley floor width to height ratio. This ratio is described by the following formula:

$$V_f = \frac{2V_{fw}}{(E_{ld} - E_{sc}) + (E_{rd} - E_{sc})}$$

In this formula,  $V_{fw}$  is the width of the valley floor,  $E_{ld}$  and  $E_{rd}$  are the height of the right and left slopes (from water level), and  $E_{sc}$  represents the height of the valley floor (Bull and McFadden, 1977; Bull 1977). The  $V_f$  values vary linked to the shape of the valley. If “V”-shaped valleys have low  $V_f$  values, this indicates the regional uplift rate is high and there is excavation occurring (Bull and McFadden 1977; Rockwell et al., 1984; Silva et al., 2003; El Hamdouni et al., 2008). Contrarily if there are high  $V_f$  values, the uplift rate is low indicating that tectonism is less effective compared to erosional processes.

In this study the  $V_f$  values in fluvial channels were calculated for mountain fronts. Thus, the aim was to distinguish tectonic classes based on relative activities and uplift rates according to segment and to allow discussion (Rockwell et al., 1984; Silva et al., 2003; Bull, 2007).

The  $V_f$  values calculated for 37 different drainage basins within the Başkale basin varied from 0.2 to 2.6 (Table 2, Figure 5a). The valleys of the SE-flowing streams in the footwall perpendicular to the Ziraniş fault controlling the west edge of Başkale basin and valleys of streams flowing along the Erek and Albayrak faults controlling the central section of the basin offer low  $V_f$  values (valleys forming controlled by S2 and S4-S7, Table 2, Figure 5a). The valleys in these areas are V-shaped. The valleys developing linked to segments controlling the east edge of the basin appear to have higher  $V_f$  values (S8-S10, Table 1, Figure 5a). From the  $V_f$  values it may be said that the segments controlling the west edge and the northeast of the Başkale basin are more active compared to other segments.

Studies in recent years have stated there is a correlation between the  $V_f$  index and  $S_{mf}$  index and that the degree of activity of faults may be determined linked to this ratio (Rockwell et al., 1984; Silva et al., 2003). Linked to this classification, the Ziraniş and Işıklı faults (S1,S2) controlling the basin have active mountain fronts and appear to be faults with high activity controlling the basin (Figure 5b). At the same time, segments located in the northeast of the basin and those controlling the central section of the basin (S4-7) are younger and may be said to have high activity

Table 2- Valley floor width to height ratio ( $V_f$ ) values (for points see figure 5).

| Valley | $V_f$ | Valley | $V_f$ |
|--------|-------|--------|-------|
| 1a     | 0,30  | 4c     | 1,05  |
| 1b     | 0,28  | 5a     | 0,45  |
| 1c     | 0,62  | 5b     | 0,35  |
| 1d     | 0,57  | 6a     | 0,52  |
| 1e     | 0,34  | 6b     | 0,31  |
| 1f     | 0,24  | 6c     | 0,35  |
| 1g     | 0,41  | 7a     | 0,48  |
| 2a     | 0,31  | 7b     | 0,69  |
| 2b     | 1,01  | 7c     | 0,52  |
| 2c     | 0,20  | 8a     | 0,55  |
| 2d     | 0,32  | 9a     | 2,60  |
| 2e     | 2,16  | 9b     | 0,67  |
| 3a     | 0,92  | 9c     | 1,74  |
| 3b     | 1,97  | 10a    | 0,87  |
| 3c     | 2,63  | 10b    | 0,61  |
| 3d     | 1,26  | 10c    | 1,29  |
| 3e     | 2,70  | 10d    | 0,82  |
| 3f     | 2,58  | 10e    | 1,44  |
| 4a     | 2,17  | 10f    | 0,69  |
| 4b     | 0,81  | 10g    | 1,02  |

(Figure 5b). The Çamlık Fault controlling the east edge of the basin provided higher  $V_f$  and  $S_{mf}$  values. This fault appears to be moderately active compared to other faults. The uplift rate linked to these values in the west and north of Başkale basin (S1, S2, S4-7) is  $>0.5 \text{ mm yr}^{-1}$ , while moving toward the east this rate appears to be 0.05 and  $0.5 \text{ mm yr}^{-1}$  (Figure 5b).

### 3.3. Asymmetry Factor, (AF)

The drainage basin asymmetry index is one of the easiest ways to understand whether a drainage network developed under tectonic control. This index is described by this formula.

$$AF = 100 \frac{(Ar)}{(At)}$$

Here,  $Ar$  is the area to the right of the drainage basin while  $At$  is the total area of the drainage basin. If a region is under tectonic control, the best results are understood from the texture and geometry developing within the fluvial network. To define this and determine the tendency toward tectonic control, this index is used (Keller and Pinter, 2002). If the AF value is around 50,

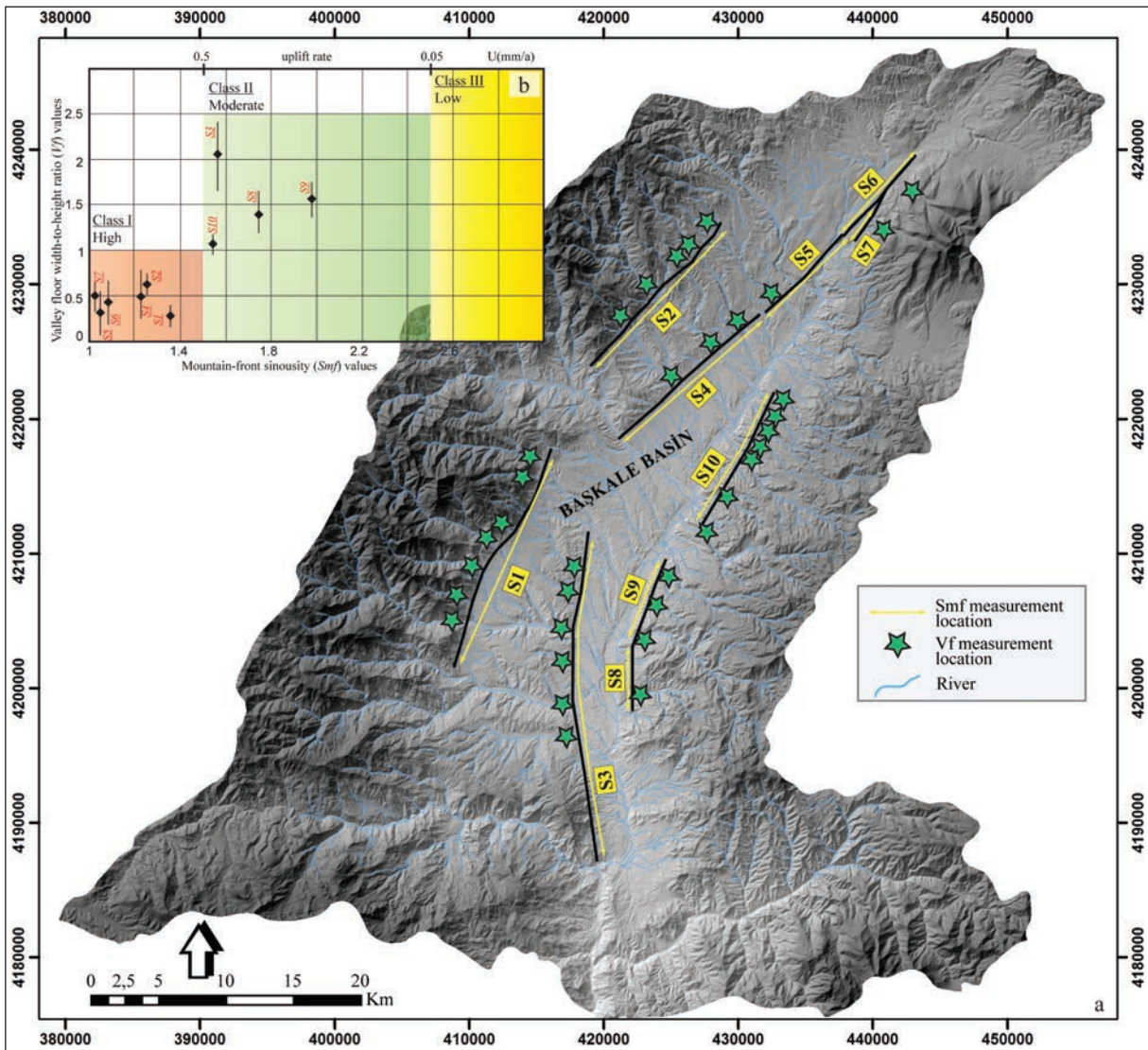


Figure 5- a) Location of  $S_{mt}$  and  $V_f$  measurements in Başkale basin b) Graphic appearance of  $S_{mt}$  and  $V_f$  values calculated for each segment and representative tectonic classes (uplift rates taken from Rockwell et al., 1984).

it indicates there is no tendency in the basin; in other words there is no tectonism affecting the basin. If this value is “ $AF > 50 < AF$ ”, it shows the basin was affected by tectonism. The drainage basin asymmetry value was calculated for 89 different basins and sub-basins controlled by the Başkale Fault Zone.

Some researchers in recent years have stated that when the AF value is taken as an absolute function, this value shows the direction of asymmetry and that basin asymmetry may be collected in four classes linked to this value. These are symmetric basin ( $AF < 5$ ), basin with low symmetry ( $5 < AF < 10$ ), basin with moderate asymmetry ( $10 < AF < 15$ ) and basin with dominant asymmetry ( $AF > 15$ ) (Perez-Peña et al., 2010; Giaconia et al., 2012).

The asymmetry factor was calculated for 20 sub-basins located within Başkale basin (Figure 6). Of these basins, 12 were symmetric-low symmetric basins while 8 were within the asymmetric basin classification. The sub-basins at the southwest edge of the basin were symmetric-low symmetric, while those toward the northwest were dominantly asymmetric. It is thought that this basin symmetry difference in the north and south sections of the west edge of the basin is due to lithology. In the south section the basement rocks are dominantly marble-schist intercalations, while the volcanic and fluvial deposits that outcrop in the central and northern sections are more easily eroded and this may have caused them to gain asymmetric character. The sub-basins in the east of the basin are in the asymmetric class in the central

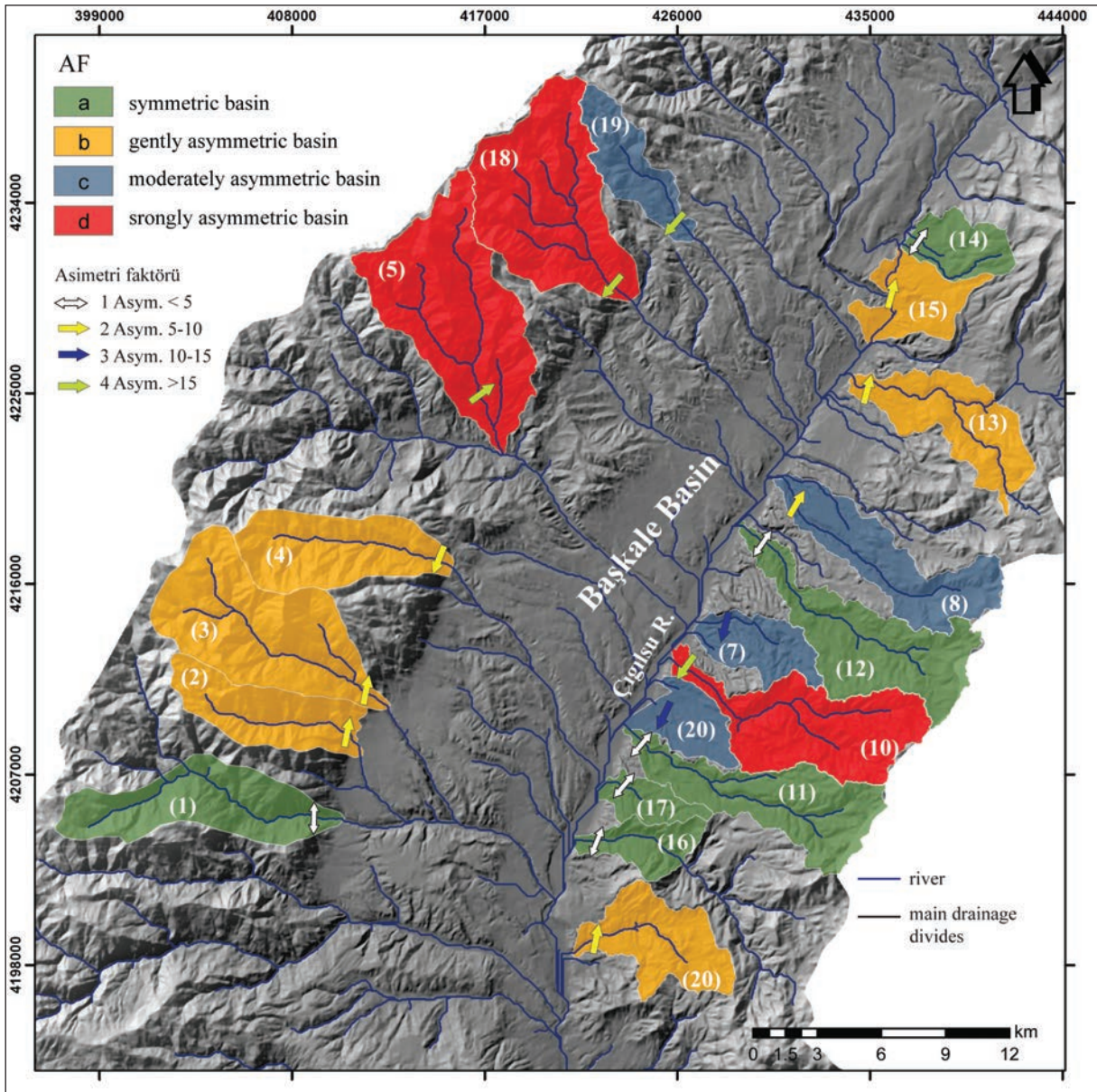


Figure 6- Asymmetry of drainage basins in sub-basins of the Başkale basin.

section, while toward the southeast and northeast the sub-basins are symmetric-low symmetric (Figure 6).

The sub-basins controlled by the Işıklı Fault in the west section of the basin have an asymmetry toward the northwest, while the sub-basins controlled by the Ziraniş Fault have an asymmetry toward the south-southwest (Figure 6). The sub-basins controlled by the Çamlık Fault in the south do not show any tendency, while those in the central section have a tendency toward the south-southwest. Sub-basins controlled by Çamlık Fault in the north have an asymmetry toward the north-northeast (Figure 6).

The asymmetry directions for sub-basins located within the Başkale basin display differences in orientation. The Başkale basin and the BFZ controlling development of this basin are located in the area between the right-lateral strike-slip Guilato–Siahcheshmeh–Khoy and Yüksekova fault zones (Figure 2). At the same time, according to block models linked to GPS data, the Hakkari block located within the Başkale basin is moving in an anti-clockwise direction (Reilinger et al., 2006; Djamour et al., 2011). The effect of these two right-lateral strike-slip fault zones controlling the main tectonic evolution of the region on the Başkale basin and BFZ has led



to the different directions of asymmetry in the sub-basins.

#### 3.4. Hypsometric curve and integral (HE and HI)

Hypsometric analysis shows the sensitivity of drainage evolution in an area to current tectonism and this analysis has been commonly used in geomorphology, hydrology and active tectonic areas in recent years (Ciccacci et al., 1992; Lifton and Chase, 1992; Ohmori, 1993; Willgoose, 1994; Willgoose and Hancock, 1998; D'Alessandro et al., 1999; Chen et al., 2003; Yıldırım, 2014; Özkaymak, 2015; Özsayın, 2016). This analysis comprises two stages; hypsometric curve and integral. The shape of the hypsometric curve (HE) is linked to the degree of excavation within a basin. While convex-shaped HE characterize immature, weakly eroded basins, S-shaped HE indicate moderately eroded basins and concave-shaped HE indicate very eroded basins (Keller and Pinter, 2002; Pérez-Peña et al., 2009a; Giaconia et al., 2012). Hypsometric integral values represent young basins if larger than 0.5 ( $HI > 0.5$ ), while values lower than 0.3 ( $HI < 0.3$ ) indicate old basins. If the value is  $0.3 < HI < 0.5$ , it shows the basin has completed formation. In this study the hypsometric curve and integral values were calculated using the CalHypso program (Pérez-Peña et al., 2009a, b) working within the ArcGIS program.

The hypsometric curves and hypsometric integrals were calculated for 20 sub-basins within the Başkale basin. The sub-basins located on the west slope of the basin are generally convex and S-shaped, with HI values larger than 0.35. The basins in the west edge of the basin, especially, controlled by the Işıklı and Ziraniş segments dominantly display convex HE, while moving toward the north along their extensions S-shaped basins are observed (Figure 7a). It may be said that basins in this area are younger linked to the hypsometric curves of the sub-basins. On the east slope, the sub-basins in the south section of the Çamlık segment display dominantly convex and S-shaped hypsometric curves (Figure 7a-c). Moving toward the north, the presence of concave basins is noted (Figure 7a, d). The sub-basins in this area are younger than those in the south, while those in the north appear to have completed their basin development. However, the volcanic units outcropping in the northeast of Başkale basin are more easily abraded and eroded, which may lead to concave hypsometric curves in these basins.

#### 4. Discussion and Conclusions

Başkale basin, located in the southeast of Van province, is one of the basins formed in the neotectonic period controlled by NE-striking left-lateral strike-slip faults with normal component (Figure 2). With the aim of analyzing tectonic activity of the basin in the Quaternary period, geomorphic indices like the mountain-front sinuosity, hypsometric integral, drainage basin asymmetry and valley floor width to height ratio were used for morphometric calculations along the BFZ controlling the basin and these results are correlated with segments of the BFZ.

Shown as an active fault on Turkey's Active Fault Map updated in 2012 (Emre et al., 2012) and controlling Başkale basin, the BFZ is a left-lateral strike-slip fault with normal component. It comprises three main fault segments. The clearest morphological lineations are the Işıklı and Ziraniş faults bounding the northwest of the basin and dipping southeast, the Çamlık Fault located on the eastern edge of the basin dipping west, and the Ereğ and Albayrak faults located in the central section of the basin forming stepped geometry toward the basin. The current morphotectonic activity of the BFZ is visible in offset stream beds, fault-controlled drainage systems (like Çığlısuyu stream), alluvial fans parallel to faults with deformation, fault terraces, hot springs and fissure ridge travertine formation that continues today.

Some researchers have proposed that geomorphological analyses provide important information to use in comparing the uplift rates in a region (Rockwell et al., 1984; Mayer, 1986; Silva et al., 2003; Bull, 2007). The researchers divided uplift rate into three different classes linked to  $V_f$  and  $S_{mf}$  values;  $>0.5 \text{ mm yr}^{-1}$  (class 1) for tectonically active mountain fronts,  $0.05\text{--}0.5 \text{ mm yr}^{-1}$  (class 2) for moderate mountain fronts and  $<0.05 \text{ mm yr}^{-1}$  (class 3) for inactive mountain fronts (Figure 5b).  $S_{mf}$  and  $V_f$  values were calculated for each segment controlling the Başkale basin. The degree of activity and uplift rates of segments linked to these values were analyzed. According to the findings, the uplift rate of segments controlling the west edge of Başkale basin is  $>0.5 \text{ mm yr}^{-1}$  and these are within class 1 (active) (Figure 5b). On the eastern edge, this uplift rate is between  $0.05$  and  $0.5 \text{ mm yr}^{-1}$  with the segments controlling this area located within class 2 (moderately active) (Figure 5b). According to block modeling linked to GPS data, the Hakkari block located within Başkale basin is

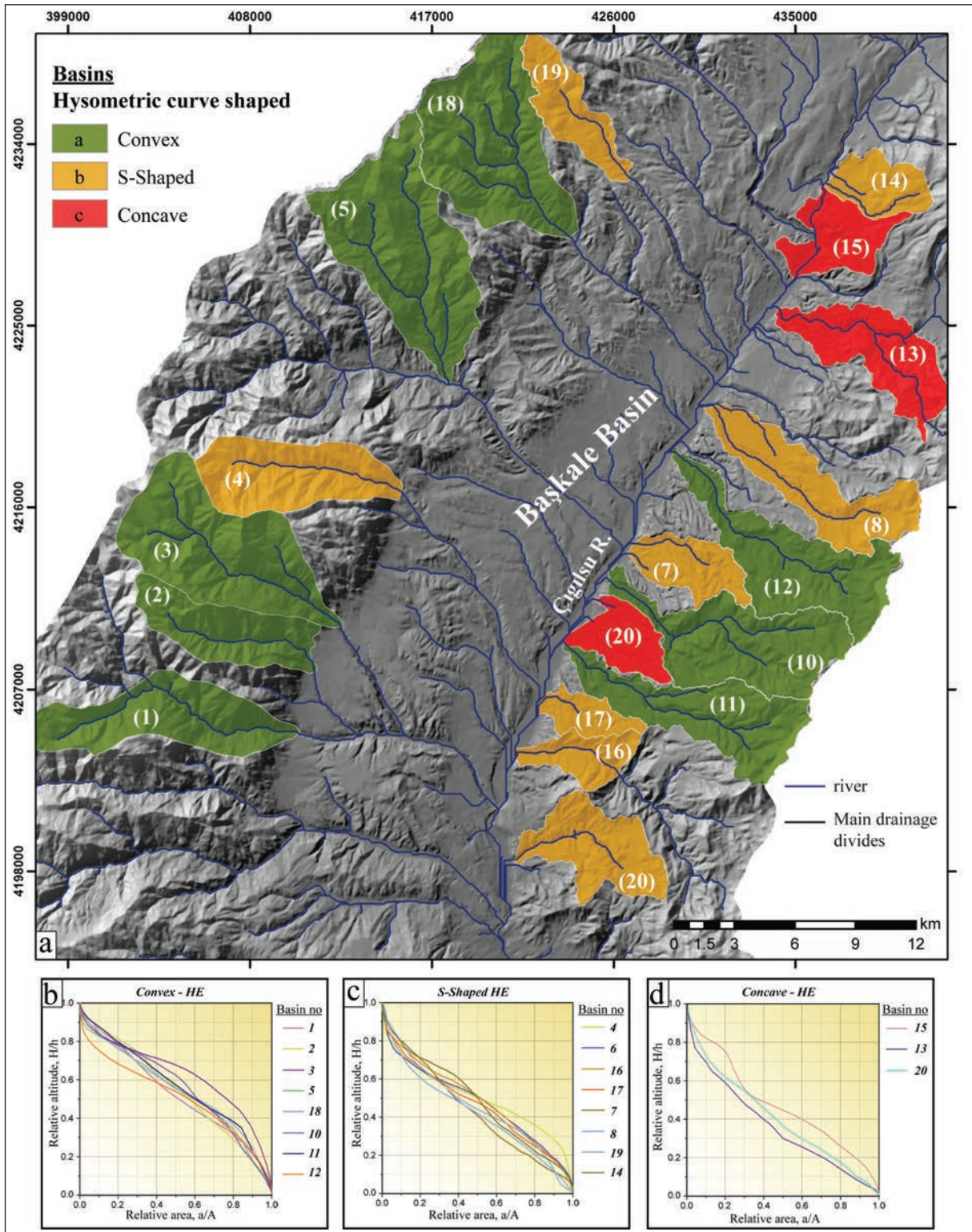


Figure 7- a) Classification linked to hypsometric curve and integral values of sub-basins within the Başkale Basin, b), c), and d) graphs of the hypsometric curves for the sub-basins.

moving in an anticlockwise direction (Reilinger et al., 2006; Djamour et al., 2011). Due to this motion, the west sections of the basin appear to have greater uplift rates, while moving to the east these uplift rates may be said to reduce. In short, the results of analyses show the uplift rates increase in the Hakkâri block from east to west.

Drainage basin asymmetry, hypsometric curves and integral values for 20 sub-basins located within the Başkale basin show the sub-basins on the west edge of the basin are generally young and asymmetric. The Ziraniş and Işıklı faults controlling these basins actively control the region and this shows the basins have a tendency toward asymmetry. However, when the direction of asymmetry is examined, the sub-basins on the Işıklı Fault tend toward the northeast, while the sub-basins on the Ziraniş Fault tend toward the southwest (Figure 6). Similarly, basins in the northern section of the Çamlık Fault tend toward the northeast, while moving to the south there is no asymmetry observed. The difference in asymmetry directions in these sub-basins is thought to be due to the tectonics of the region not just being controlled by the BFZ but also by the Guilato–Siahcheshmeh–Khoy and Yüksekova fault zones.

When HE and HI values are considered, it appears that the west and southeast edges of the basin are formed of young sub-basins. The sub-basins southeast of the Işıklı, Ziraniş and Çamlık faults especially provide high HI integral values. However, though the sub-basins on both slopes of the basin generally have different types of HE and HI values, the sub-basins controlled by the Işıklı, Ziraniş and Çamlık (southeast section) faults, especially are young, while the sub-basins in the northeast section of the Çamlık Fault appear older (Figure 7). This data shows the development of the Başkale basin was controlled by the Işıklı and Ziraniş faults along the west edge of the basin.

In conclusion, in light of findings obtained from digital elevation models, the Başkale Fault Zone is a left-lateral strike-slip fault with normal component. The morphological elements developed within Başkale basin appear to be controlled by the BFZ. The fault plains developing in front of the Işıklı and Ziraniş Faults controlling the west edge of Başkale basin and the secondary stepped faults cutting these fault plains show they advance toward the east of the basin. Morphometric analysis results show the area has a very young topography and is actively uplifting.

The uplift rate in the region increases from east to west and in western sections is determined to be more than 0.5 mm per year.

### Acknowledgements

The authors wish to thank Prof. Dr. Hasan Sözbilir and Prof. Dr. Ercan Aksoy for contributions to the review process of this study.

### References

- Altner, Y., Söhne, W., Güney, C., Perl, J., Wang, R., Muzli M. 2013. A geodetic study of the 23 October 2011 Van, Turkey earthquake. *Tectonophysics*, 588, 118-134.
- Ambraseys, N.N. 2001. Reassessment of earthquakes, 1900-1999, in the Eastern Mediterranean and the Middle East. *Geophysical Journal International* 145, 471-487, doi:10.1046/j.0956-540x.2001.01396.x/epdf
- Ambraseys, N.N., Finkel, A.C. 1995. The seismicity of Turkey and adjacent areas: A historical review, 1500-1800. M.S. Eren Beyoğlu, Istanbul.
- Arpat, E., Şaroğlu, F., İz, H.B. 1977. 1976 Çaldıran Depremi. *Yeryuvarı and İnsan* 17, 29-41.
- Ateş, Ş., Mutlu, G., Özerk, O.Ç., Çiçek, İ., Karakaya Gülmez, F., Bulut Üstün, A., Karabıyıköğlu, M., Osmañcelebioğlu, R., Özata, A., Aksoy, A. 2007. Van İlinin Yerbilim Verileri, Maden Tetkik ve Arama Genel Müdürlüğü, Rapor no: 10961. 152s Ankara (unpublished).
- Azor, A., Keller, E.A., Yeats, R.S. 2002. Geomorphic indicators of actiand fold growth: South Mountain-Oak Ridge anticline, Andntura basin, southern California. *Bulletin of the Geological Society of America* 114, 745-753.
- Bayraktar, A., Altunışık, A.C., Pehlivan M. 2013. Performance and damages of reinforced concrete buildings during the October 23 and November 9, 2011 Van, Turkey, earthquakes. *Soil Dynamics and Earthquake Engineering*, 53, 49-72.
- Boray, A. 1975. Bitlis dolayının yapısı ve metamorfizması. *Türkiye Jeoloji Bülteni*, 18, 81-84.
- Bull, W.B. 1977. Tectonic geomorphology of the Mojaand Desert, California, U.S. Geological Surandy Contract Report 14-0-001-G-394.
- Bull, W.B. 2007. Tectonic Geomorphology of Mountains: A New Approach to Paleoseismology. Wiley-Blackwell, USA.

- Bull, W.B., McFadden, L.D. 1977. Tectonic geomorphology north and south of the Garlock fault, California. *Geomorphology in Arid Regions*, 115-138.
- Chen, Y.C., Sung, Q., Cheng, K.Y. 2003. Along-strike variations of morphotectonic features in the Western Foothills of Taiwan: Tectonic implications based on stream-gradient and hypsometric analysis. *Geomorphology* 56, 109-137, doi:10.1016/S0169-555X(03)00059-X.
- Ciccacci, S., D'Alessandro, L., Fredi, P., Palmieri, E.L. 1992. Relations between morphometric characteristics and denudational processes in some drainage basins of Italy. *Zeitschrift fur Geomorphologie* 36, 53-67.
- Cisternas, A., Philip, H., Bousquet, J. C., Cara, M., Deschamps, A., Dorbath, L., Tatevossian, R. 1989. The Spitak (Armenia) earthquake of 7 December 1988: Field observations, seismology and tectonics. *Nature*, 339(6227), 675-679, doi:10.1038/339675a0.
- D'Alessandro, L., Del Monte, M., Fredi, P., Lupia-Palmeri, E., Peppoloni, S. 1999. Hypsometric analysis in the study of Italian drainage basin morphoevolution. *Transactions, Japanese Geomorphological Union* 20, 187-202.
- Dewey, J.F., Hempton, M.R., Kidd, W.S.F., Saroğlu, F., Şengör, A.M.C. 1986. Shortening of continental lithosphere: The neotectonics of Eastern Anatolia - A young collision zone. *Geological Society Special Publication*, pp. 1-36.
- Dhont, D., Chorowicz, J. 2006. Review of the neotectonics of the Eastern Turkish-Armenian Plateau by geomorphic analysis of digital elevation model imagery. *International Journal of Earth Sciences* 95, 34-49.
- Djamour, Y., Andriant, P., Nankali, H.R., Tavakoli, F. 2011. NW Iran-eastern Turkey present-day kinematics: Results from the Iranian permanent GPS network. *Earth and Planetary Science Letters*, 307, 27-34, doi:10.1016/j.epsl.2011.04.029.
- Doğan, B., Karakaş, A. 2013. Geometry of co-seismic surface ruptures and tectonic meaning of the 23 October 2011 M w 7.1 Van earthquake (East Anatolian Region, Turkey). *Journal of Structural Geology*, 46, 99-114, doi:10.1016/j.jsg.2012.10.001.
- El Hamdouni, R., Irigaray, C., Fernández, T., Chacón, J., Keller, E.A. 2008. Assessment of tectonic and tectonics, southwest border of the Sierra Nevada (southern Spain). *Geomorphology* 96, 150-173, doi:10.1016/j.geomorph.2007.08.004.
- Elliott, J.R., Copley, C., Holley, R., Scharer, K., Parsons, B. 2013. The 2011 Mw 7.1 Van (Eastern Turkey) earthquake. *Journal of Geophysical Research: Solid Earth*, 118, 1619-1637.
- Emre, Ö., Doğan, A., Özalp, Ö., Yıldırım, Y. 2005. 25 Ocak 2005 Hakkari Depremi Hakkında Ön Değerlendirme. *Maden Tetkik ve Arama Genel Müdürlüğü. Rapor No: 123. Ankara (unpublished)*
- Emre, Ö., Duman, T.Y., Özalp, S., Olgun, Ş., Elmacı, H. 2012. 1:250.000 ölçekli Türkiye diri fay haritaları serisi, Van (NJ38-5) Paftası, Seri No:52, Maden Tetkik ve Arama Genel Müdürlüğü, Ankara-Türkiye.
- Erdoğan, T. 1975. Gölbaşı Civarının Jeolojisi. TPAO. Rapor, 929, 18.
- Ergin, K., Güçlü, U., Uz, Z. 1967. Türkiye ve civarının deprem kataloğu (MS. 11-1964). İstanbul, İTÜ, Maden Fakültesi, Arz Fiziği Enstitüsü yayınları.
- Font, M., Amorese, D., Lagarde, J.L. 2010. DEM and GIS analysis of the stream gradient index to evaluate effects of tectonics: The Normandy intraplate area (NW France). *Geomorphology* 119, 172-180, doi:10.1016/j.geomorph.2010.03.017.
- Giaconia, F., Booth-Rea, G., Martínez-Martínez, J.M., Azañón, J.M., Pérez-Peña, J.V. 2012. Geomorphic analysis of the Sierra Cabrera, an actiand pop-up in the constrictional domain of conjugate strike-slip faults: The Palomares and Polopos fault zones (eastern Betics, SE Spain). *Tectonophysics* 580, 27-42, doi:10.1016/j.tecto.2012.08.028.
- Giamboni, M., Wetzel, A., Schneider, B. 2005. Geomorphic response of alluvial riandrs to actiand tectonics: Example from the southern Rhine Graben. *Aust. J. Earth Sci.* 97, 24-37.
- Gordon, R.G. 1998. The plate tectonic approximation: plate nonrigidity, diffuse plate boundaries, and global plate reconstructions. *Annual Review of Earth and Planetary Sciences*, pp. 615-642, doi:10.1146/annurev.earth.26.1.615.
- Göncüoğlu, M. C., Turhan, N. 1984. Geology of the Bitlis metamorphic belt. *Maden Tetkik Arama yayınları* (In: Tekeli, O. ve Göncüoğlu, M.C. (eds), 237-244.
- Görgün, E. 2013. The 2011 October 23 M-W 7.2 Van-Ercis, Turkey, Earthquake And Its Aftershocks", *Geophysical Journal International*, 1052-1067.
- Gürbüz, A., Gürer, Ö. F. 2008. Tectonic geomorphology of the north Anatolian Faultzone in the Lake Sapanca Basin (eastern Marmara region, Turkey). *Geosciences Journal*, 12(3), 215-225.

- Horasan, G., Boztepe-Güney, A. 2006. Observation and analysis of low frequency crustal earthquakes in Lake Van and its vicinity, eastern Turkey Journal Seismology. 11, 1-13. doi:10.1007/s10950-006-9022-2
- Karakhanian, A.S., Trifonov, V.G., Philip, H., Avagyan, A., Hessami, K., Jamali, F., Bayraktutan, M.S., Bagdassarian, H., Arakelian, S., Davtian, V., Adilkhanyan, A., 2004. "Active faulting and natural hazards in Armenia, eastern Turkey and northwestern Iran", Tectonophysics, 380, 189–219.
- Keller, E. A. 1986. Investigation of active tectonics: Use of surficial Earth processes. In R. E. Wallace (Ed.), Active tectonics (pp. 136–147). Washington, DC: National Academy Press. Studies in Geophysics.
- Keller, E. A. Seaandr, D.B., Laduzinsky, D.L., Johnson, D.L., Ku, T.L., 2000. Tectonic geomorphology of actiand folding oandr buried reandrse faults: San Emigdio Mountain front, Southern San Joaquin Valley, California. Bulletin of the Geological Society of America 112, 86-97, doi:10.1130/0016-7606(2000)112%3C86:TGOAFO%3E2.0.CO;2.
- Keller, E. A. Pinter, N., 2002. Actiand Tectonics, Prentice Hall, New Jersey.
- Koçyiğit, A. 1985a. Karayazi Fayı. Yerbilimleri, 28, 67-72.
- Koçyiğit, A. 1985b. Muratbast - Balabantas (Horasan) arasında Çobandede Fay kuşağının jeotektonik özellikleri ve Horasan-Narman depremi yüzey kırıkları. Cumhuriyet Üniversitesi, Mühendislik Fakültesi Dergisi, 2, 17-33.
- Koçyiğit, A. 2005. Sütlice (Hakkari) Depreminin Kaynağı: Başkale Fay Kuşağı, GD Türkiye) Deprem Sempozyumu, Denizli, Turkey.
- Koçyiğit, A. 2013. New field and seismic data about the intraplate strike-slip deformation in Van region, East Anatolian plateau, E. Turkey. Journal of Asian Earth Sciences 62, 586-605, doi:10.1016/j.jseaes.2012.11.008.
- Koçyiğit, A., Yılmaz, A., Adamia, S., Kuloshvili, S. 2001. Neotectonic of East Anatolian Plateau (Turkey) and Lesser Caucasus: Implication for transition from thrusting to strike-slip faulting. Geodinamica Acta 14, 177-195, doi:10.1016/S0985-3111(00)01064-0.
- KOERI, 2011. KOERI (Boğaziçi Üniversitesi Kandilli Rasathanesi ve Deprem Araştırma Enstitüsü), 2011 - 2012 (<http://www.koeri.boun.edu.tr/scripts/Ist5.asp>)
- Lifton, N.A., Chase, C.G. 1992. Tectonic, climatic and lithologic influences on landscape fractal dimension and hypsometry: implications for landscape evolution in the San Gabriel Mountains, California. Geomorphology 5, 77-114, doi:10.1016/0169-555X(92)90059-W.
- Mayer, L. 1986. Tectonic geomorphology of escarpments and mountain fronts. Actiand Tectonics, 125-135.
- Ohmori, H. 1993. Changes in the hypsometric curand through mountain building resulting from concurrent tectonics and denudation. Geomorphology 8, 263-277, doi:10.1016/0169-555X(93)90023-U.
- Özkaymak, Ç., Sözbilir, H., Bozkurt, E., Dirik, K., Topal, T., Alan, H., Çağlan, D. 2011. 23 Ekim 2011 Tabanlı-Van Depreminin Sismik Jeomorfolojisi ve Doğu Anadolu'daki Aktif Tektonik Yapılarla Olan İlişkisi. JMO Jeoloji Mühendisliği Dergisi 35 (2) 175-199.
- Özkaymak, Ç., Sözbilir, H. 2012. Tectonic geomorphology of the Spildağı high ranges, western Anatolia. Geomorphology, 173–174, 128–140.
- Özkaymak, Ç. 2015. Tectonic analysis of the Honaz Fault (western Anatolia) using geomorphic indices and the regional implications. Geodinamica Acta, 27:2-3, 110-129.
- Özsayın, E. 2016. Relative tectonic activity assessment of the Çameli Basin, Western Anatolia, using geomorphic indices, Geodinamica Acta, doi: 10.1080/09853111.2015.1128180.
- Pérez-Peña, J.V., Azañón, J.M., Azor, A. 2009a. CalHypso: An ArcGIS extension to calculate hypsometric curands and their statistical moments. Applications to drainage basin analysis in SE Spain. Computers and Geosciences 35, 1214-1223, doi:10.1016/j.cageo.2008.06.006.
- Pérez-Peña, J.V., Azañón, J.M., Booth-Rea, G., Azor, A., Delgado, J. 2009b. Differentiating geology and tectonics using a spatial autocorrelation technique for the hypsometric integral. Journal of Geophysical Research: Earth Surface 114.
- Pérez-Peña, J.V., Azor, A., Azañón, J.M., Keller, E.A. 2010. Actiand tectonics in the Sierra Nevada (Betic Cordillera, SE Spain): Insights from geomorphic indexes and drainage pattern analysis. Geomorphology 119, 74-87, doi:10.1029/2008JF001092.
- Rebai, S., Philip, H., Dorbath, L., Borissoff, B., Haessler, H., Cisternas, A. 1993. Active tectonics in the lesser Caucasus: coexistence of compressive and extensional structures. Tectonics, 12(5), 1089-1114, doi:10.1029/93TC00514.

- Reilinger, R., McClusky, S., Andriant, P., Lawrence, S., Ergintav, S., Cakmak, R., Ozener, H., Kadirov, F., Guliev, I., Stepanyan, R. 2006. GPS constraints on continental deformation in the Africa-Arabia-Eurasia continental collision zone and implications for the dynamics of plate interactions. *Journal of Geophysical Research: Solid Earth* (1978–2012) 111, doi:10.1029/2005JB004051.
- Ricou, L. 1971. Le croissant ophiolitique péri-arabe: Une ceinture de nappes mises en place au Crétacé supérieur.
- Rockwell, T.K., Keller, E.A., Johnson, D.L. 1984. Tectonic geomorphology of alluvial fans and mountain fronts near Andntura, California. *Tectonic Geomorphology*, 183-207.
- Silva, P.G., Goy, J.L., Zazo, C., Bardají, T., 2003. Fault-generated mountain fronts in southeast Spain: Geomorphologic assessment of tectonic and seismic activity. *Geomorphology* 50, 203-225, doi:10.1016/S0169-555X(02)00215-5.
- Soysal, H., Sipahioğlu, S., Koçak, D., Altınok, Y. 1981. Türkiye ve Çevresinin Tarihsel Deprem Kataloğu (MÖ 2100-MS 1900). TUBİTAK Projesi (TBAG), Ankara:.
- Strahler, A.N. 1952. Hypsometric (area-altitude) analysis of erosional topography. *Bulletin of the Geological Society of America* 63, 1117-1142.
- Şaroğlu, F., Yılmaz, G., Erdoğan, R. 1984. "Horasan-Narman depreminin jeolojik özelliği ve Doğu Anadolu'da depreme yönelik çalışmaların gerekliliği", *Kuzeydoğu Anadolu I. Ulusal Deprem Sempozyumu. Atatürk Üniversitesi, Erzurum*, 349-360.
- Şaroğlu, F., Yılmaz, Y. 1986. Doğu Anadolu'da neotektonik dönemdeki jeolojik evrim and havza modelleri. *Maden Tektik ve Arama Dergisi*, 107, 73-94.
- Şaroğlu, F., Emre, Ö., Boray, A. 1987. Türkiye'nin diri fayları ve depremsellikleri. *Maden Tetkik ve Arama Genel Müdürlüğü. Report No: 5216*.
- Şengör, A.M.C., Kidd, W.S.F. 1979. Post-collisional tectonics of the Turkish-Iranian plateau and a comparison with Tibet. *Tectonophysics* 55, 361-376, doi:10.1016/0040-1951(79)90184-7.
- Şengör, A. M. C., Yılmaz, Y. 1981. Tethyan evolution of Turkey: A plate tectonic approach. *Tectonophysics*, 75(3-4), 181-190,193-199,203-241, doi:10.1016/0040-1951(81)90275-4.
- Şengör, A.M.C., Görür, N., and Şaroğlu, F., 1985. Strike-slip faulting and related basin formation in zones of tectonic escape: Turkey as a case study.
- Tan, O., Tapirdamaz, M.C., Yörük, A. 2008. "The earthquake catalogues for Turkey", *Turkish Journal of Earth Sciences*, 17(2), 405-418.
- Willgoose, G. 1994. A statistic for testing the elevation characteristics of landscape simulation models. *Journal of Geophysical Research* 99, 13987-13996, doi:10.1029/94JB00123.
- Willgoose, C., Hancock, G. 1998. Revisiting the hypsometric curand as an indicator of form and process in transport-limited catchment. *Earth Surface Processes and Landforms* 23, 611-623.
- Yıldırım, C. 2014. Relative tectonic activity assessment of the Tuz Gölü fault zone; Central Anatolia, Turkey. *Tectonophysics*, 630, 183–192.
- Yılmaz, O. 1975. Casas Bölgesi (Bitlis Masifi) kayaçlarının petrografik ve stratigrafik incelenmesi. *Türkiye Jeoloji Bülteni*, 18-1, 33-40.
- Yılmaz, Y. 1971. Etüde petrographique et geochronologique de la region de Casa (Partie Meridionale du Masif de Bitlis, Turquie, These de doct 3 cycle). *Univ. Sci.Med. Greonable*, 230.
- Yılmaz, Y., Şaroğlu, F., Güner, Y. 1987. Initiation of the neomagmatism in East Anatolia. *Tectonophysics* 134, 177-199, doi:10.1016/0040-1951(87)90256-3.